EPSC Abstracts
Vol. 6, EPSC-DPS2011-1630, 2011
EPSC-DPS Joint Meeting 2011

Observations of thermal emission from the south pole of Enceladus in August 2010

J. R. Spencer (1), C. J. A. Howett (1), A. J. Verbiscer (2), T. A. Hurford (3), M. E. Segura (3), and J. C. Pearl (3)
(1) Southwest Research Institute, 1050 Walnut St. Suite 300, Boulder CO 80302, (2) Dept. of Astronomy, University of Virginia, Charlottesville, VA 22904, (3) NASA-Goddard Space Flight Center, Greenbelt, MD 20771.

Abstract

The Cassini CIRS instrument continues its observations of the thermal emission from the active "tiger stripe" fractures at the south pole of Enceladus. On August 13th 2010, on orbit 136, the "E11" Enceladus encounter provided a particularly favorable geometry for remote sensing of the south pole, and yielded some of the most detailed observations of tiger stripe thermal emission of the entire mission. Maps of 6.7 – 16.7 µm thermal emission from one of the brightest regions of Damascus Sulcus reveal large variations in brightness along the length of the fracture with a peak near the source of Plume 2 [7]. The emission from the brightest region is close to a blackbody, with best-fit temperatures in the range 167 – 185 K, depending on the exact wavelength range and spatial subset of the data that is fitted. Lower-temperature radiation is also seen from the flanks of the sulcus.

1. Introduction

Endogenic thermal emission from the active "tiger stripe" fractures [5] in the south polar region of Enceladus was discovered by the Composite Infrared Spectrometer (CIRS) instrument on the Cassini spacecraft [2] during Cassini's July 2005 flyby of Enceladus [6]. Those initial observations were limited in wavelength coverage (9 – 16 µm only) and spatial resolution (complete coverage at 25 km resolution, plus sparsely scattered observations at 6 km resolution). Subsequent flybys have greatly improved our knowledge of the thermal emission. CIRS has obtained many spectral image cubes using its "FP3" (9 – 17 µm, 600 – 1100 cm^{-1}) and "FP4" (7 – 9 µm, 1100 – 1500 cm^{-1}) detectors, including full south polar coverage at ~6 km resolution and maps of a few selected regions at ~1 km resolution. The "FP1" (16 – 500 µm, 20 – 600 cm^{-1}) detector also made many scans with ~10x lower spatial resolution.

The examples discussed here focus on the August 13th 2010 flyby. On this flyby, Cassini approached Enceladus on the night side from a latitude of 17 degrees south, yielding oblique nighttime views of the south polar region. Closest approach was almost directly over the south pole at a range of 2550 km, close enough to map thermal emission at sub-km resolution but distant enough to allow surface features to tracked, allowing good FP3 and FP4 maps of short-wavelength emission along Damascus Sulcus, as well as an FP1 scan of long-wavelength emission from and between the tiger stripes.

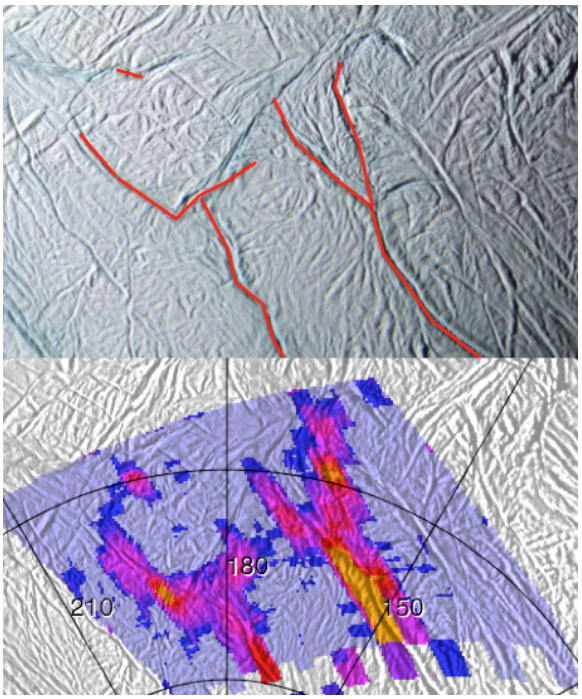

Figure 1: Complex thermal emission from a system of fractures near 180 W, 75 S observed by CIRS during the August 2010 Enceladus flyby. The upper image shows, in red, the fractures that are likely to be active, based on the observed emission pattern. NASA/JPL/SwRI/SSI

2. Spatial Distribution

The August 2010 flyby provided improved resolution (4.5 km/pixel) of a region of complex emission centered near 180 W, 75 S (Fig. 1), showing that current activity is not confined exclusively to the four parallel tiger stripes, but also involves subsidiary fractures which may be at a significant angle to the main fractures and thus subject to significantly different stress fields.

800 meter resolution mapping of the brightest part of the tiger stripe Damascus Sulcus, near the source of plume 2 [7], show that most of the emission is concentrated within 0.4 km of the center of the Sulcus. It is not possible from the CIRS data to determine whether the ~150 m total width of the emission determined from the spectral fits (Fig. 2) results from a single fracture, or multiple parallel fractures within the 0.8 km field of view of the detector. The August 2010 data show that significant emission is also present in pixels adjacent to those centered on Damascus Sulcus.

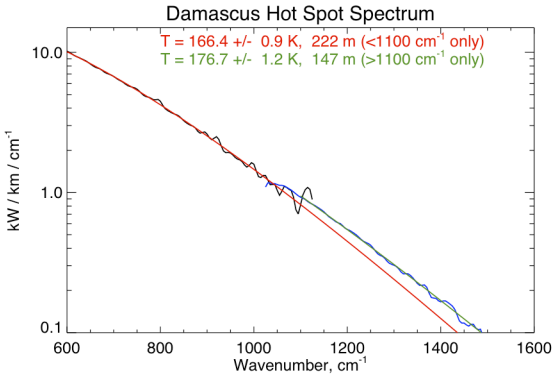

Figure 2: The spectrum of the brightest mapped part of Damascus Sulcus. The best fit blackbody (red) to the spectrum at lower wavenumbers (black) falls below the observed higher-wavenumber spectrum (blue), implying a range of temperatures in the CIRS field of view, with temperatures reaching at least as high as the 177 K best-fit to the higher-wavenumber spectrum (green). The best-fit width of a linear source along the fracture, in meters, is also shown.

3. Spectra

The combined FP3/FP4 600 – 1500 cm^{-1} (16.7 – 6.7 μm) of the brightest mapped portion of Damascus Sulcus is shown in Fig. 2. The spectrum is close to that of a blackbody, but an excess of radiation at high wavenumbers implies a distribution of temperatures within the field of view, reaching at least 177 K (the best fit temperature to the higher-wavenumber data), though spectra of some sub-regions are fit by temperatures at least as high as 185 K. Absolute fluxes show that the warm region along the fractures is at least 150 m wide. Best-fit temperatures of the flanking radiation are near 130 K, lower than in the center of the tiger stripes, and a width of 300 – 400 m.

3. Discussion:

The observed thermal emission is probably brought to the surface by the flow of vapor and ice particles that generates the plumes, along near-vertical fractures [1,3,4,6]. Most observed emission probably results from heat conducted from the fracture to the surface on either side of the fracture [1]. However, single fractures cannot easily conduct enough heat to match the emission intensity along the brightest fractures [1,3], and multiple parallel fractures may be required. Simple conductive models [1] predict that surface temperatures should drop below 100 K within 100 meters of an active fracture, and thus cannot explain the August 2010 observations of radiation from the flanks of Damascus Sulcus, which is many hundred meters from the center of the Sulcus. These new data will thus enable refinement of models for the delivery of heat to the surface, and improved constraints on subsurface conditions.

References

[1] Abramov, O. and Spencer, J. R. (2009) Icarus 199 189–196.

[2] Flasar, F. M. et al. (2004) Space Science Rev. 115 169–297.

[3] Ingersoll, A. P. and Pankine, A. A. (2010) Icarus 206 594–607.

[4] Nimmo, F. et al. (2007) Nature 447 289–291.

[5] Porco, C. P et al. (2006) Science, 311, 1393–1401.

[6] Spencer, J. R. et al. (2006) Science, 311, 1401–1405.

[7] Spitale, J. N. and Porco, C. P. (2007) Nature 449 695–697.